

Supervalent doping of LiFePO_4 with special rare earth ions: A review

Minshou Zhao^{1,3,*}, Xian Zhao² and Yuqing Qiao¹

¹College of Environmental and Chemical Engineering, Yanshan University, Qinhuangdao 066004, China,

²College of Chemistry and Chemical Engineering, Shanghai Jiaotong University, Shanghai 200240, China,

³State Key Laboratory of Metastable Material Science and Technology, Yanshan University, Qinhuangdao, Hebei 066004, China

ABSTRACT

The review addresses the work on supervalent doping of LiFePO_4 with Nd, Gd, Sm, Eu and Yb ions carried out in our group. The dopant choice, the preparation of $\text{LiFe}_x\text{M}_{1-x}\text{PO}_4$, and the effect of supervalent doping with special rare earth ions on electrochemical performance are emphasized.

KEYWORDS: cathode material, doping, rare earth element, lithium iron phosphate

INTRODUCTION

The scope of application of lithium ion battery with LiFePO_4 as cathode material is currently expanding from mobile electronic devices to electric vehicles (EVs), power tools and hybrid-electric vehicles (HEVs), and it also has attractive prospects in space and military fields. This kind of lithium-ion battery is considered as a high-capacity and high-power battery because LiFePO_4 has a higher theoretical capacity of $170 \text{ mAh}\cdot\text{g}^{-1}$ and a flat discharge voltage of 3.4V vs lithium, and has high safety characteristics and a long life cycle. LiFePO_4 also has high thermal and chemical stability and offers economic and environmental advantages, being a low cost and non-toxic material [1, 2, 3]. However, inherent poor electrical conductivity and slow lithium ion diffusivity are its obvious shortcomings [4], which result in poor

dischargeability rate, and these factors restrict its practical use. Therefore, many approaches are used to improve its electrochemical performance to meet the demands in various fields. Currently, the main methods to overcome the disadvantages mentioned above are the following: improving the synthesis process to reduce the product particle size [5] and carbon-doping [6, 7] or bulk-doping of metal ions [8], which can enhance the comprehensive performance of the resultant product. Recently doping approaches have become a hot research area.

This review addresses the research results of the recent work on LiFePO_4 carried out in our group.

1. Why some special rare earth ions?

1. According to M. Saiful Islam *et al.* [9], the energy of dopant substitution or “solution” reaction can be calculated by combining appropriate defect and lattice energy. The calculated result shows that the lowest energy for Nd^{3+} ion is found at Fe site for all aliovalent cations.
2. Among all the rare earth elements, only Gd has 7 electrons in the outermost shell which is referred to as ‘half full 4f electron shell’. The special electronic structure itself provokes interest.
3. Among all the rare earth elements, three elements, Sm, Eu, and Yb, are well known abnormal elements. They often present stable 3 valence in their compounds, but also stable 2 valence in some reductive environments.

*Corresponding author: zhaoms@ysu.edu.cn

4. Aliovalent doping or substitution for Fe site in LiFePO_4 will create many defects, which enhance electrochemical activity of LiFePO_4 , and then improve the electrochemical performance.
5. Aliovalent doping or substitution for Fe site seems to result in non-balance of charge in LiFePO_4 . However, aliovalent dopant charge is balanced by lithium vacancies, with the total charge on the iron site being + 2.000 (± 0.006) [10].

Therefore, it is expected that doping LiFePO_4 with these special rare earth ions mentioned above may improve the comprehensive performance of LiFePO_4 and its special electrochemical properties.

2. Preparation of $\text{LiFe}_{1-x}\text{M}_x\text{PO}_4/\text{C}$ composite

$\text{LiFe}_{1-x}\text{M}_x\text{PO}_4$ ($\text{M} = \text{Nd, Gd, Sm, Eu}$ and Yb ; $x = 0, 0.01, 0.02, 0.04, 0.06, 0.08$) compounds were synthesized by two-step heating solid-state reaction. $\text{CH}_3\text{COOLi}\cdot 2\text{H}_2\text{O}(\text{AR})$, $\text{FeC}_2\text{O}_4\cdot 2\text{H}_2\text{O}(\text{AR})$, $\text{NH}_4\text{H}_2\text{PO}_4(\text{AR})$ and M_2O_3 (purity of 99.9 mass %) were mixed according to the stoichiometric amount of LiFePO_4 , using 5 mass % glucose as the reductive agent and carbon source. Milling (ball-to-powder weight ratio of 15:1) was carried out for 8 hr, using anhydrous ethanol as dispersing agent under the argon atmosphere. The powder material was ground and compressed into a pellet after the anhydrous ethanol was evaporated. It was preheated at 400°C for 6 hr and then calcined at 700°C for 16 hr in the series resistance furnace. All these heat treatments were carried out under nitrogen atmosphere.

3. Sample characterization

Thermogravimetric analysis of all kinds of precursors was conducted in a Pyris Diamond TG/DSC apparatus in the temperature range from 40°C to 810°C . The structure of all kinds of powder samples was analyzed by X-ray diffraction (XRD) in RIGAKU D/max-2500/pc. The sample morphology was observed by a field-emission scanning electron microscope (FE-SEM) in S-4800 FE-SEM equipped with an energy dispersive spectroscopy (EDS), which was used to analyze the elemental composition. The distribution of the material particle size was measured by ZetaPAL

laser particle size analyzer. The electrochemical performance has been measured using galvanostatic charge/discharge and EIS methods. The magnetic measurement of LiFePO_4/C sample was performed by SQUID on a Magnetic Property Measurement System (SQUID) XL-7.

4. Cathode preparation, cell assembly and charge/discharge test

The electrode was prepared by dispersing 80 mass % active material, 15 mass % acetylene black and 5 mass % polyvinylidene fluoride (PVdF) in 1-methyl-2-pyrrolidinone (NMP) to form a slurry. The slurry was then coated onto an Al foil substrate (the electro-active material of about $1.5 \text{ mg}\cdot\text{cm}^{-2}$), dried under the infrared light, cut into pieces and weighted, and finally dried at 120°C for 16 hr in a vacuum drying oven. The cells were assembled in an argon-filled glove box, and the cathode film and the lithium metal foil anode were separated by a microporous polypropylene (Celgard 2400) separator containing a liquid electrolyte of 1M LiPF_6 in 1:1(vol.) EC/DMC. The cells were charged and discharged on electrochemical testing BTS-5V 10 mA, and the voltage range was between 4.2 V and 2.5 V.

5. Aliovalent doping with Neodymium or substitution for Fe sites

Hu *et al.* [11] reported that the discharge capacity and electric conductivity of LiFePO_4 have been improved significantly after doping with neodymium ion, which was synthesized by hydrothermal method and mixed with glucose as carbon source. Doping some ions in LiFePO_4 bulk to enhance the electric conductivity gave rise to much controversy. As recognized, coating carbon on the particle surface of LiFePO_4 can increase the electric conductivity. Zhao *et al.* recently reported in detail the effect of neodymium aliovalent substitution on the structure and electrochemical performance of LiFePO_4 [12].

5.1. TG-DSC analysis

Fig. 1 shows three obvious weight loss regions. The first one between 150°C and 230°C is related to the dehydration of the hydrates. The second one between 230°C and 300°C is related to the anaerobic thermal decomposition of glucose and the

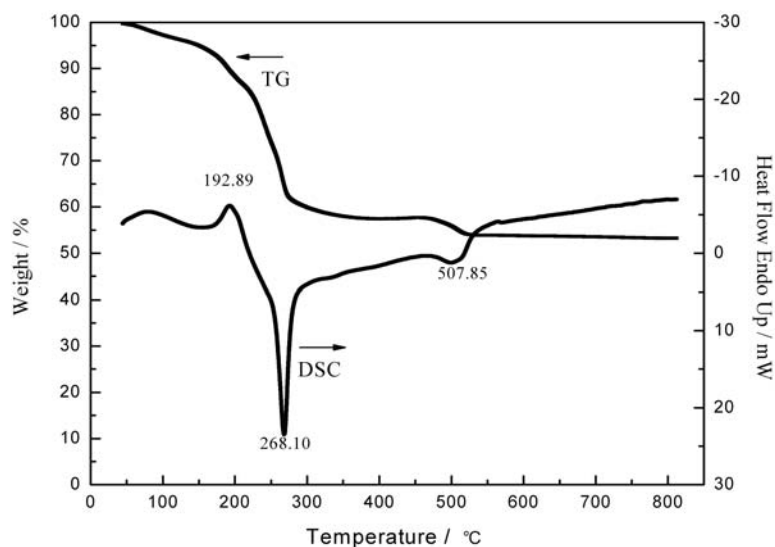


Fig. 1. TG-DSC analysis curve of $\text{LiFe}_{0.94}\text{Nd}_{0.06}\text{PO}_4/\text{C}$ precursor.

decomposition of FeC_2O_4 and $\text{NH}_4\text{H}_2\text{PO}_4$. The third one between 470°C and 560°C should concern complete decomposition of residual glucose, FeC_2O_4 and $\text{NH}_4\text{H}_2\text{PO}_4$. The corresponding DSC curve shows a smaller endothermic peak at 192.89°C and two exothermic peaks. The obvious one locates at 268.10°C which is related to the formation of LiFePO_4 compound, and the other smaller one is between 470°C and 560°C where a new solid-state reaction with the transformation of crystalline structure occurs, as indicated in literature [13]. Therefore, the choice of temperature higher than 600°C to synthesize the target product is reasonable and feasible.

Oxidation of Fe^{2+} ion into Fe^{3+} ion should be avoided and the content of Fe^{3+} ion in LiFePO_4 should be decreased as much as possible during the experiment process, because the existence of Fe^{3+} ion would seriously affect the electrochemical performance of LiFePO_4/C . Therefore, it is imperative to explore the appropriate synthesis process. In our group, SQUID is used to measure the magnetic property of Fe^{3+} in the sample. Fig. 2 shows the measured magnetization curve of LiFePO_4/C by us. The curve is a straight line if the impurity phases, which are ferromagnetic or ferrimagnetic do not exist, whereas, non-linear behaviour will be observed at low-magnetic field if the impurity phases that are ferromagnetic or

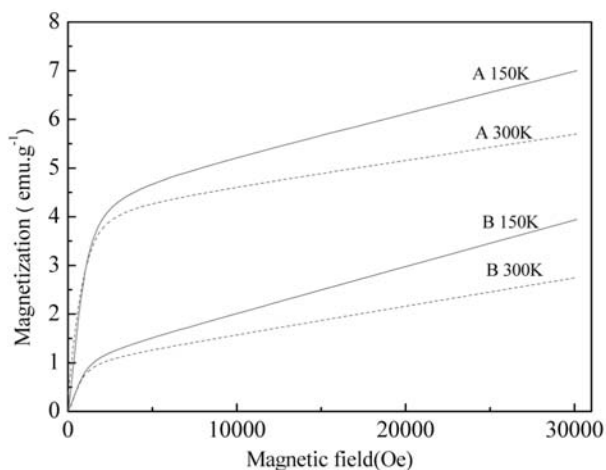


Fig. 2. Magnetization curve of LiFePO_4/C .

ferromagnetic exist [14, 15]. That is to say that the non-linear extent reflects the content of the impurity phases. Therefore, it is concluded from Fig. 2 that the sample B, which was calcined at 700°C for 16 hr, contains less content of the impurity phases than the sample A, which was calcined at 700°C for 16 hr. Here, the synthesis process used for sample B is preferable.

5.2. XRD pattern

The diffraction peak position and relative intensity of the $\text{LiFe}_{0.94}\text{Nd}_{0.06}\text{PO}_4/\text{C}$ sample is almost the same as LiFePO_4 , as shown in Fig. 3 and no impurity

peak is observed, which suggests that the small amount of Nd^{3+} -doped does not change the olivine crystal structure of LiFePO_4 . In addition, carbon diffraction peak is not observed in Fig. 4, which implies that the addition of micro-carbon also does not affect the crystal structure of LiFePO_4 .

5.3. FE-SEM and EDS analysis

Fig. 4 is FE-SEM image of LiFePO_4 , LiFePO_4/C and $\text{LiFe}_{0.94}\text{Nd}_{0.06}\text{PO}_4/\text{C}$. It can be seen from

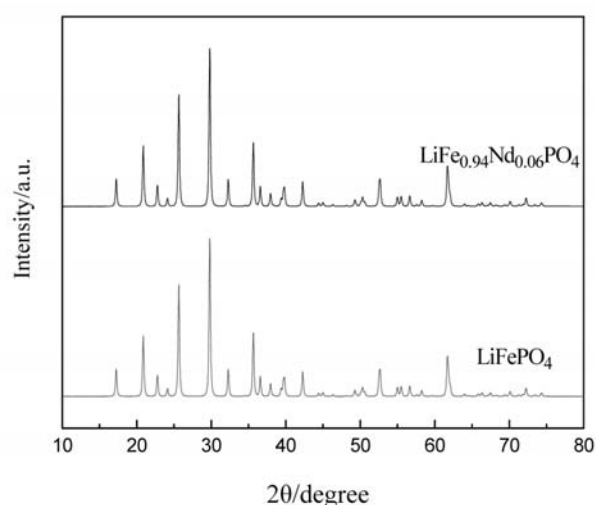


Fig. 3. XRD images of LiFePO_4 and $\text{LiFe}_{0.94}\text{Nd}_{0.06}\text{PO}_4/\text{C}$.

(a) and (b) that the particle size is refined after adding a small amount of glucose which can be completely decomposed in the calcination process. During calcination process carbon is generated and can inhibit the generation of Fe^{3+} and can be coated on LiFePO_4 to prevent it from conglomeration. It is apparent from Fig. 4 (b) and (c) that the particle size of $\text{LiFe}_{0.94}\text{Nd}_{0.06}\text{PO}_4/\text{C}$ (about 150 nm) is significantly smaller than that of LiFePO_4/C (about 400 nm), which indicates that doping small amount of Nd^{3+} ion can effectively reduce the particle size of LiFePO_4 .

The EDS analysis image of $\text{LiFe}_{0.94}\text{Nd}_{0.06}\text{PO}_4/\text{C}$ is shown in Fig. 5. The compositions of substitution element are listed in Table 1.

Combined with XRD, these results indicate that Nd^{3+} occupies Fe site in LiFePO_4 or has been dissolved into the LiFePO_4 .

5.4. Electrochemical performance

As shown in Fig. 6, 7, and 8, $\text{LiFe}_{0.96}\text{Nd}_{0.06}\text{PO}_4$ delivers the maximum discharge capacity of $165.2 \text{ mAh}\cdot\text{g}^{-1}$, $146.8 \text{ mAh}\cdot\text{g}^{-1}$, $125.7 \text{ mAh}\cdot\text{g}^{-1}$, $114.8 \text{ mAh}\cdot\text{g}^{-1}$ at 0.2 C, 1 C, 2 C, 5 C rates, respectively, and the capacity retention rate is 92.8% after 100 cycles. Fig. 9 indicates that using PZS as carbon source for coating on the surface of LiFePO_4 is more beneficial for the cycle stability than glucose.

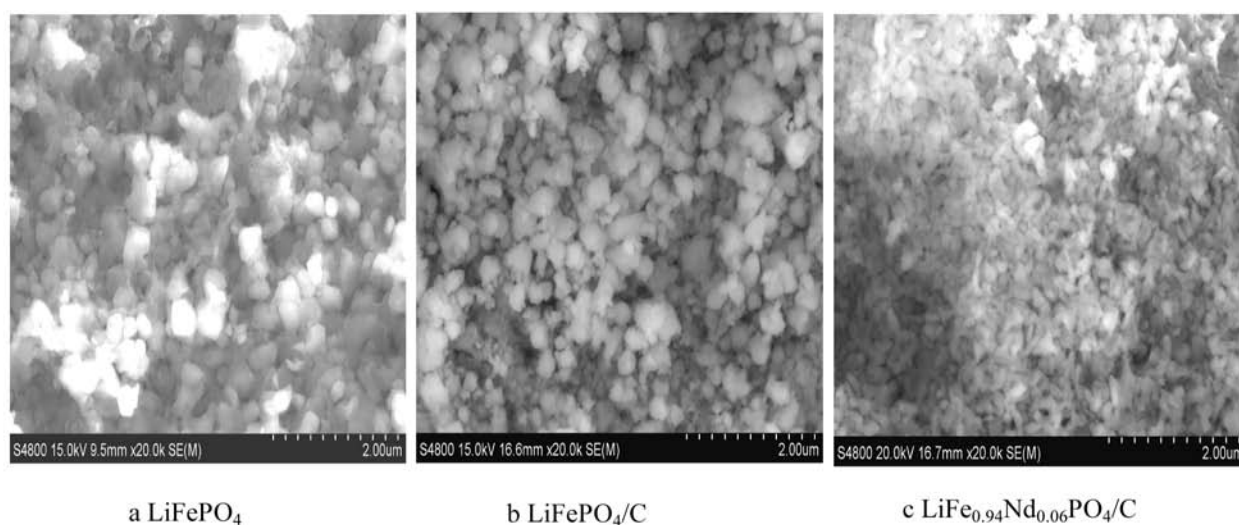


Fig. 4. FE-SEM image of LiFePO_4 , LiFePO_4/C and $\text{LiFe}_{0.94}\text{Nd}_{0.06}\text{PO}_4/\text{C}$.

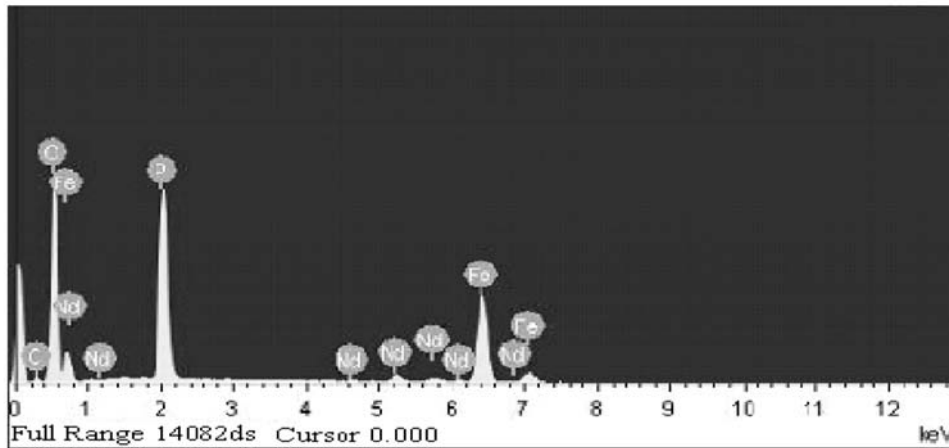


Fig. 5. EDS image of LiFe_{0.94}Nd_{0.06}PO₄/C.

Table 1. Composition of substitution element in LiFe_{0.94}Nd_{0.06}PO₄/C.

Elt	C K	O K	P K	Fe K	Nd L	Total
W / %	6.07	46.75	17.14	25.98	4.07	100.00
A / %	11.29	65.31	12.37	10.40	0.63	100.00

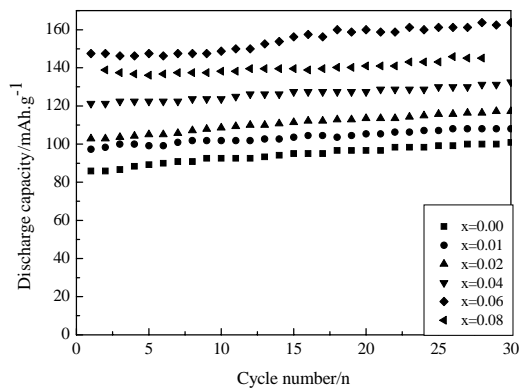


Fig. 6. Discharge capacity as a function of cycle number for LiFe_{1-x}Nd_xPO₄/C (X=0~0.08) at 0.2 C rate.

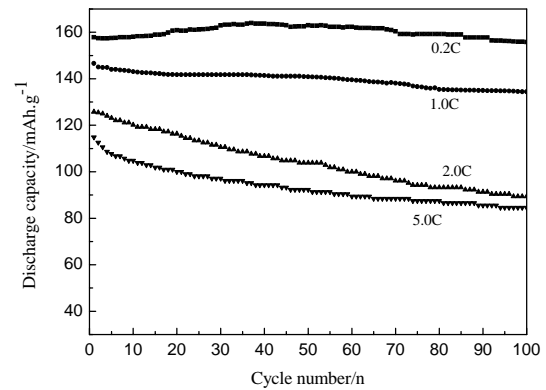


Fig. 7. Discharge capacity as a function of cycle number for LiFe_{0.94}Nd_{0.06}PO₄/C at different rates.

6. Aliovalent doping gadolinium or substitution for Fe site

6.1. XRD

Fig. 10A and Fig. 10B show the XRD pattern of LiFePO₄/C composite and Rietveld refinement of the XRD pattern for LiFe_{0.93}Gd_{0.07}PO₄/C composite [16], respectively. The observed pattern and calculated pattern match well in Fig. 10B.

The crystal phases of two samples are olivine structures indexed by orthorhombic Pnma. These results suggest that a small amount of Gd³⁺ ion-doped does not affect the olivine structure of LiFePO₄. In addition, a carbon diffraction peak is not observed in Fig. 10A and Fig. 10B, which implies that the micro-carbon coating does not affect the structure of LiFePO₄ also.

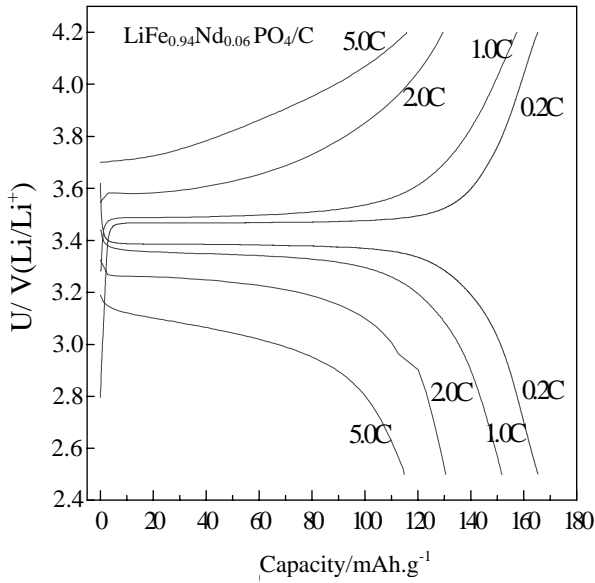


Fig. 8. Initial charge-discharge curve of $\text{LiFe}_{0.94}\text{Nd}_{0.06}\text{PO}_4/\text{C}$ at different rates.

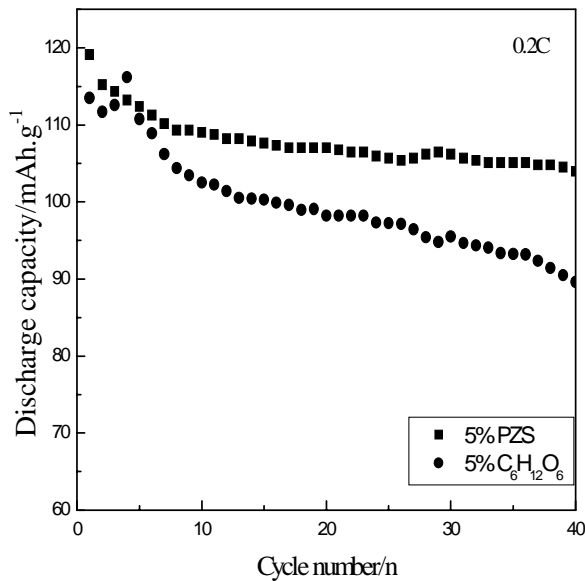


Fig. 9. Influence of different carbon source on cycle stability LiFePO_4/C at a rate of 0.2C.

However, XRD pattern of Gd-doped LiFePO_4 shows more Bragg reflections than Gd-free LiFePO_4 because the ionic radius of Gd^{3+} ion doped (0.0938 nm) is larger than that of Fe^{2+} ion (0.078 nm), leading to bigger unit cell parameters, as shown in Table 2. Table 2 lists the

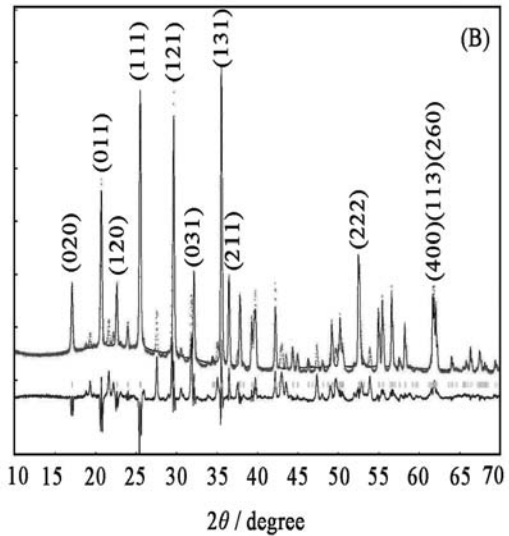
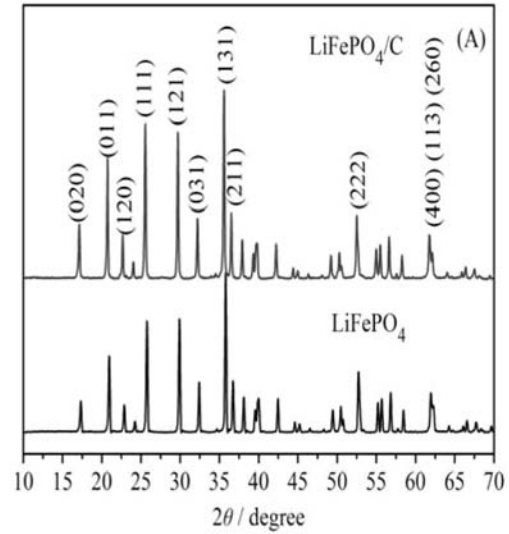


Fig. 10. (A) XRD of LiFePO_4 and LiFePO_4/C and (B) Rietveld refinement of XRD for $\text{LiFe}_{0.93}\text{Gd}_{0.07}\text{PO}_4/\text{C}$.

Table 2. Unit cell parameter obtained from XRD Rietveld refinement of XRD for $\text{LiFe}_{0.93}\text{Gd}_{0.07}\text{PO}_4/\text{C}$ and unit cell parameter of LiFePO_4/C .

Sample	a(nm)	b(nm)	c(nm)
LiFePO_4/C	1.0324	0.6007	0.4695
$\text{LiFe}_{0.93}\text{Gd}_{0.07}\text{PO}_4/\text{C}$	1.0471	0.6092	0.4758

unit cell parameter obtained from Rietveld refinement of the XRD for $\text{LiFe}_{0.93}\text{Gd}_{0.07}\text{PO}_4/\text{C}$ and unit cell parameter of LiFePO_4/C . Results of Rietveld refinement confirm that Gd^{3+} ion has

been successfully doped into the LiFePO₄/C. Clearly, doping a small amount of Gd³⁺ ion has little effect on the cell parameters of LiFePO₄, and the dopant of a larger ionic radius perhaps creates more defects in LiFePO₄, which is beneficial for the electrochemical catalytic activity of the electrode.

6.2. Particle size, FE-SEM and EDS

The grain size of samples can be described by particle size distribution. Fig. 11 presents the particle size distribution histogram of LiFePO₄/C sample and LiFe_{0.93}Gd_{0.07}PO₄/C sample, respectively. Fig. 12 depicts the FE-SEM images of LiFePO₄/C and LiFe_{0.93}Gd_{0.07}PO₄/C, respectively. It is apparent from Fig. 11 and Fig. 12 that the particle size of LiFe_{0.93}Gd_{0.07}PO₄/C sample is significantly smaller

than that of LiFePO₄/C sample, and the particle scale is uniform after doping Gd³⁺ ion, which indicates that doping a small amount of Gd³⁺ can effectively reduce the particle size of LiFePO₄/C and make it more uniform.

The EDS image of LiFe_{0.93}Gd_{0.07}PO₄/C is shown in Fig. 13. The compositions of the substituent elements are listed in Table 3. The result shows the atomic ratio of Fe, Gd, P and O is 0.981: 0.067: 1: 4.858 in LiFe_{0.93}Gd_{0.07}PO₄/C sample, essentially coinciding with LiFe_{0.93}Gd_{0.07}PO₄/C. The supervalent-cation dopant in LiFePO₄ is studied by combining neutron and X-ray diffraction. The results showed that low levels of dopants were indeed soluble in the olivine lattice up to the extent of 3 mol %. Therefore, we infer that Gd³⁺ ion occupies Fe²⁺ ion site in LiFePO₄/C

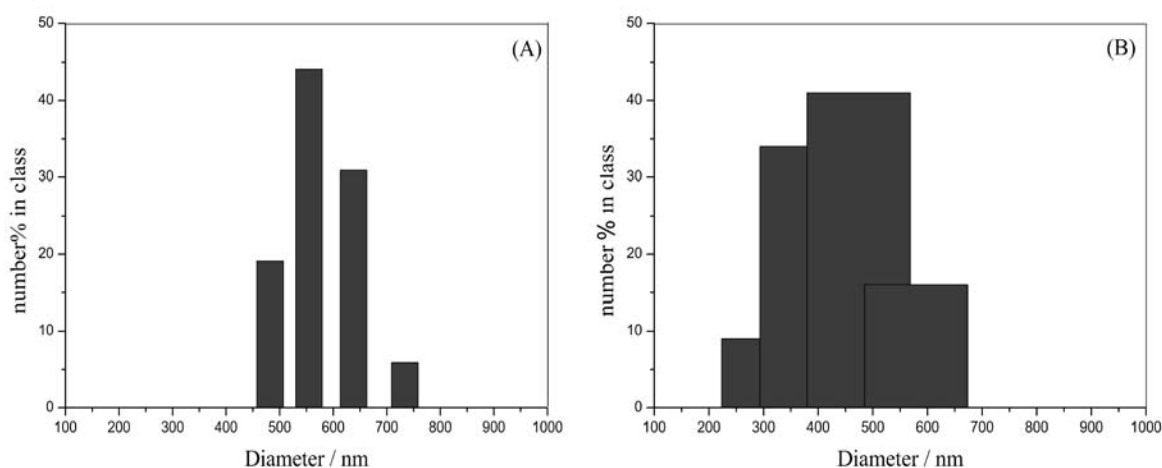


Fig. 11. (A) particle size distributions of LiFePO₄/C and (B) particle size distributions of LiFe_{0.93}Gd_{0.07}PO₄/C.

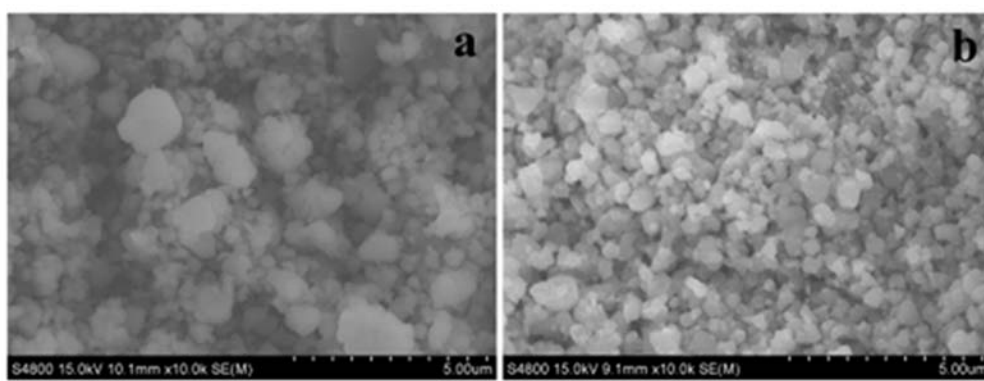


Fig. 12. FE-SEM images of LiFePO₄/C (a) and LiFe_{0.93}Gd_{0.07}PO₄/C (b).

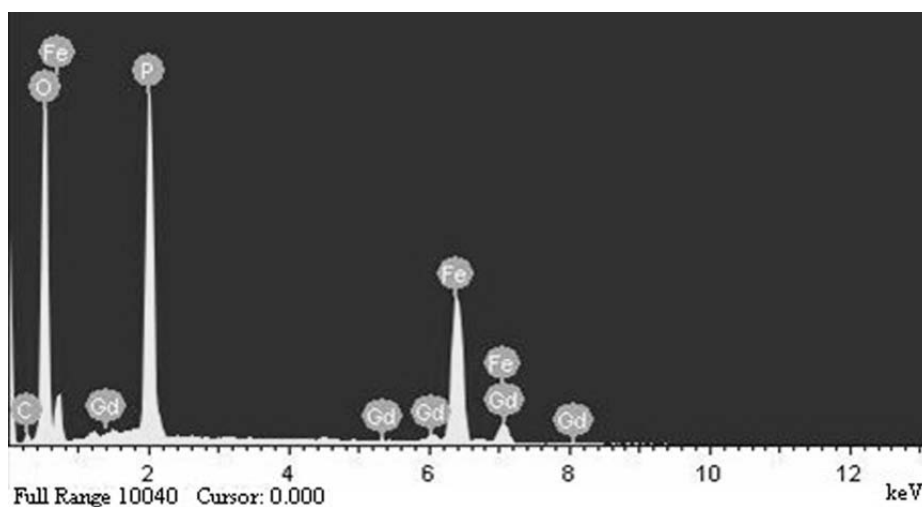


Fig. 13. EDS image of $\text{LiFe}_{0.93}\text{Gd}_{0.07}\text{PO}_4/\text{C}$.

Table 3. Element composition in $\text{LiFe}_{0.93}\text{Gd}_{0.07}\text{PO}_4/\text{C}$.

Elt	C K	O K	P K	Fe K	Gd L	Total
W %	5.40	42.23	16.83	29.77	5.77	100.00
A %	10.71	62.81	12.93	12.68	0.87	100.00

or has been dissolved into LiFePO_4/C to form a solid solution.

6.3. Electrochemical performance

The cycle performance of $\text{LiFe}_{0.93}\text{Gd}_{0.07}\text{PO}_4/\text{C}$ sample at various rates is shown in Fig. 14(A). The maximum discharge capacity is 150.7 mAh g^{-1} , 125.9 mAh g^{-1} , 106.0 mAh g^{-1} and 81.3 mAh g^{-1} at rates of 0.2 C, 1 C, 5 C and 10 C, respectively. Fig. 14(B) shows the discharge curves of $\text{LiFe}_{0.93}\text{Gd}_{0.07}\text{PO}_4/\text{C}$ sample at various rates. It is concluded that doping an appropriate amount of Gd^{3+} ion can improve the high-rate discharge performance of LiFePO_4/C composite.

It is inferred that doping Gd^{3+} ion can reduce the particle size of LiFePO_4/C , shorten the transport path of Li^+ ion, increase the disorder of the lattice and create the defect in LiFePO_4/C . These factors would improve the electrochemical performance of LiFePO_4/C composite.

The electrochemical measurements have also been carried out at lower temperatures, as shown in Fig. 15. And at 0.1 C rate, the initial discharge

capacity is 122.2 mAh g^{-1} , 107.7 mAh g^{-1} , 80.4 mAh g^{-1} and 66.3 mAh g^{-1} at 0°C , -10°C , -20°C and -30°C , respectively. The discharge capacity monotonously sharply decreases with decreasing temperature, just as expected. At lower temperature the transport speed of Li^+ ion slows down and ohmic polarization influence becomes more dominant. These perhaps are key issues to influence discharge capability.

EIS was used to further analyze the effect of doping Gd^{3+} ion on the electrode reaction impedance. Fig. 16 shows EIS of LiFePO_4/C electrode reaction and $\text{LiFe}_{0.93}\text{Gd}_{0.07}\text{PO}_4/\text{C}$ electrode reaction at 15°C . The results were obtained using Zview software and are listed in Table 4. The ohmic resistance (R_s) almost does not change for two samples, because the same electrolyte was used. As expected, charge-transfer impedance obviously decreases in the charge-discharge process because of the addition of Gd^{3+} ion. The charge transfer resistance (R_{ct}) for LiFePO_4/C electrode reaction and $\text{LiFe}_{0.93}\text{Gd}_{0.07}\text{PO}_4/\text{C}$ electrode reaction is 692.6Ω and 241.3Ω , respectively. This great

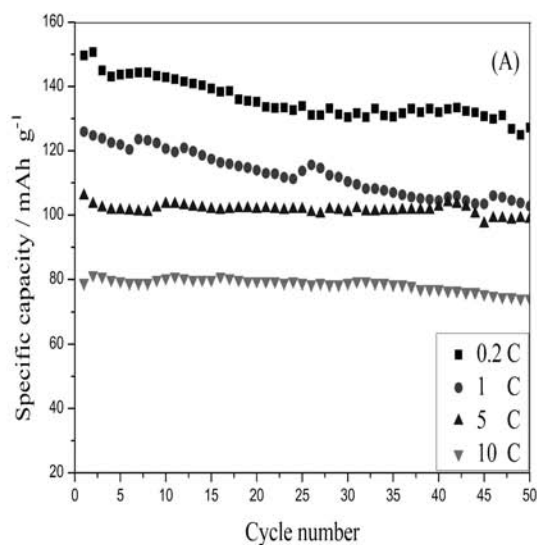


Fig. 14. (A) Discharge capacity as a function of cycle number for $\text{LiFe}_{0.93}\text{Gd}_{0.07}\text{PO}_4/\text{C}$ at various rates.

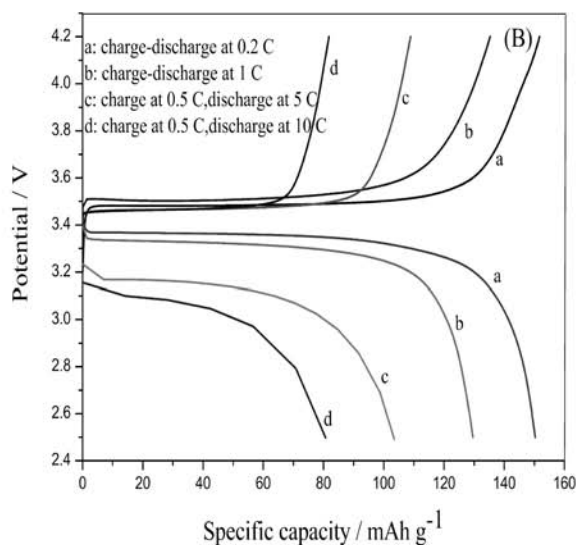


Fig. 14. (B) Second charge-discharge curves of $\text{LiFe}_{0.93}\text{Gd}_{0.07}\text{PO}_4/\text{C}$ at various rates.

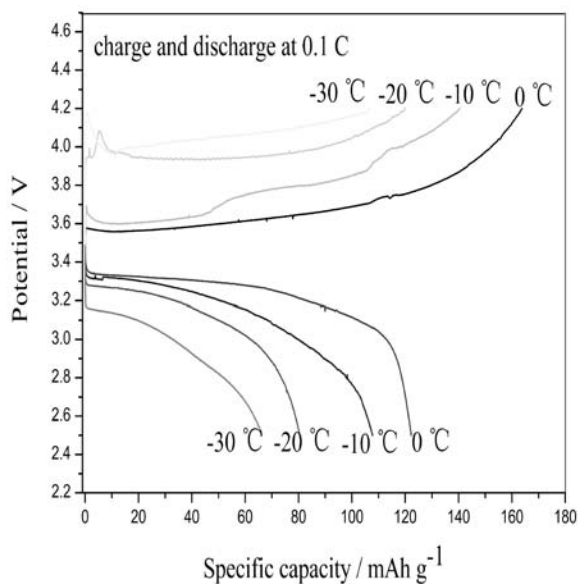


Fig. 15. Initial charge-discharge curves of $\text{LiFe}_{0.93}\text{Gd}_{0.07}\text{PO}_4/\text{C}$ at various temperatures.

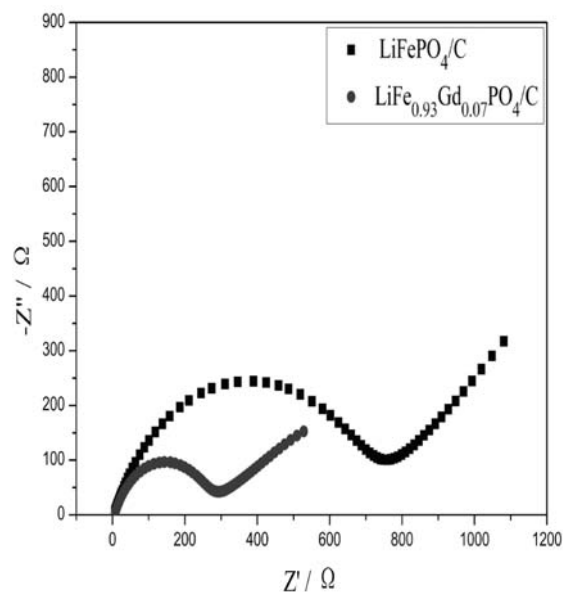


Fig. 16. EIS for LiFePO_4/C and $\text{LiFe}_{0.93}\text{Gd}_{0.07}\text{PO}_4/\text{C}$ electrode after 3 cycles.

decrease in the impedance will benefit to overcome the restriction of kinetics in the charge-discharge process and improve the cycling performance of the material.

An apparent exchange current density (I_0) can be often used to sign the catalytic activity of electrode, which is an important parameter of

Table 4. Electrochemical impedance and exchange current density.

Sample	$R_s(\Omega)$	$R_{ct}(\Omega)$	$I_0(\text{mA}\cdot\text{g}^{-1})$
LiFePO_4/C	3.406	692.6	26.3
$\text{LiFe}_{0.93}\text{Gd}_{0.07}\text{PO}_4/\text{C}$	3.288	241.3	128.5

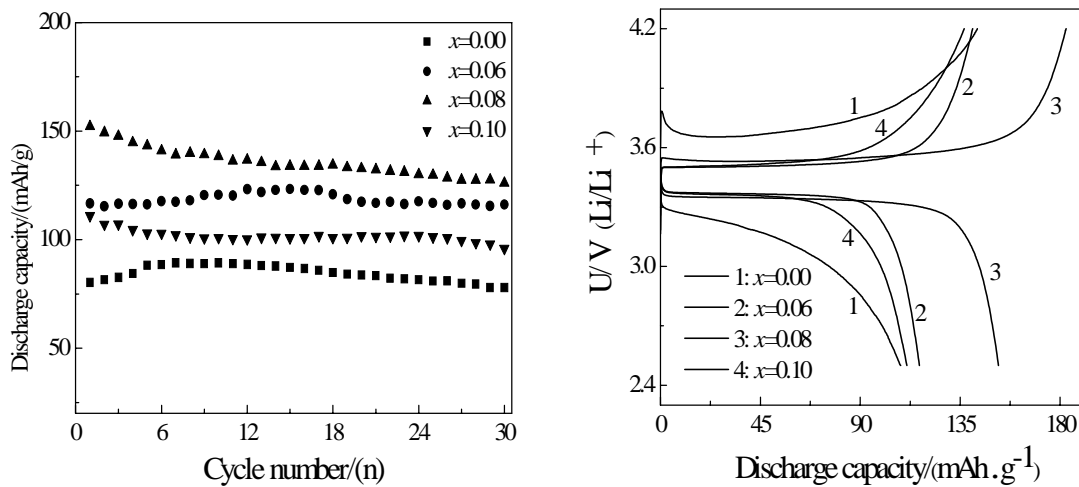


Fig.17. Cycle performances (left) and initial charge-discharge curve of $\text{LiFe}_{1-x}\text{Sm}_x\text{PO}_4/\text{C}$ (right).

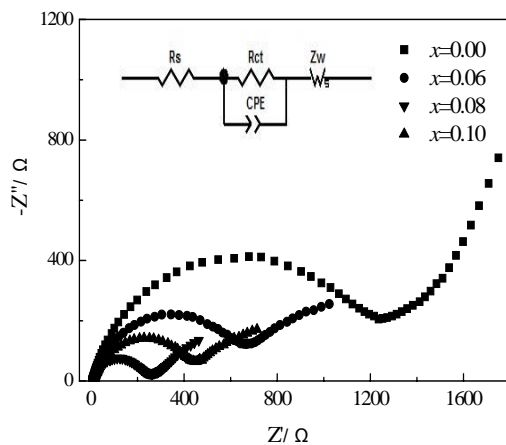


Fig. 18. EIS for $\text{LiFe}_{1-x}\text{Sm}_x\text{PO}_4/\text{C}$ ($x=0, 0.06, 0.08, 0.10$).

kinetics for an electrochemical reaction. When overpotential is very small, it can be calculated using Formula (1) [17] and the results are also listed in Table 4.

$$I_0 = R \cdot T / n R_{ct} \cdot F \quad (1)$$

where R is gas constant, T is absolute temperature, F is Faraday constant, n is charge-transfer number and R_{ct} is charge-transfer resistance.

7. Aliovalent doping abnormal rare earth (Sm, Eu, Yb) or substitution for Fe site in LiFePO_4

Compared with other rare earth elements, Sm, Eu and Yb have some unique characteristics and are

often called as abnormal rare earth elements. Based on results of Nd and Gd as dopants in LiFePO_4 , doping Sm, Eu and Yb were also carried out via the same experimental procedures as above mentioned [18, 19].

As expected, the effect of respective doping Sm, Eu and Yb in LiFePO_4 on the electrochemical performances has almost the same results and trend. The experimental results of doping Sm as a representative element have been given below.

7.1. Electrochemical performance

The cycle performance of $\text{LiFe}_{1-x}\text{Sm}_x\text{PO}_4/\text{C}$ sample and initial charge-discharge curves are shown in Fig. 17 (left) and (right), respectively. It is concluded from Fig. 17 that due to doping Sm, the discharge capacity increases and the difference of plateau gap between the charge/discharge curves become narrow, and the polarization becomes small. The rate performance has been improved because of doping Sm in LiFePO_4 , just like as influence on discharge capacity.

Fig. 18 shows EIS for $\text{LiFe}_{1-x}\text{Sm}_x\text{PO}_4/\text{C}$ ($x = 0, 0.06, 0.08, 0.10$) electrode reaction. When x equals 0.08, R_{ct} has lowest value, 199 Ω , much lower than that without doping Sm, 1211 Ω .

7.2. Temperature effect

The effect of temperature on the discharge capacity has been carried out for doping Sm at the range of -20°C to 60°C , as shown in Fig. 19.

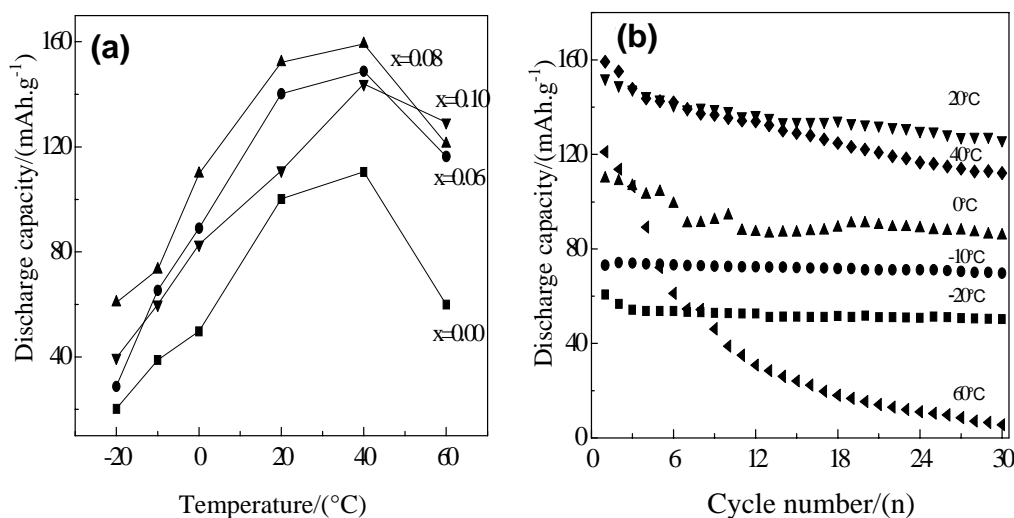


Fig. 19. (a) Discharge capacity of $\text{LiFe}_{1-x}\text{Sm}_x\text{PO}_4/\text{C}$ and (b) cycle performances of sample with $x=0.08$ at various temperature.

The relation between discharge capacity and temperature is as expected. The discharge capacity monotonously sharply decreases both at higher or lower temperature than ambient temperature.

8. There are many problems to be further investigated on doping in olivine LiFePO_4

Since 1997, more than thousand papers on LiFePO_4 cathode material for Li-ion battery have been published, and the application of LiFePO_4 as cathode material is moving forward fast and has seen the first light in commercialization. Doping some elements in LiFePO_4 is a very effective approach for the improvement of performances for LiFePO_4 . However, there are some academic problems to be investigated in future. More accurate experimental methods and compelling results are needed.

1. There are ambivalent viewpoints on dopant state in olivine lattice. Islam *et al.* reported that “on energetic ground, LiFePO_4 is not tolerant to aliovalent doping (e. g., Al, Ga, Zr, Ti, Nb, Ta) on either Li (M1) or Fe (M2) sites.” However, Wagemaker *et al.* stated that “low levels of dopants are indeed soluble in the olivine lattice up to the extent of 3 mol % (in bulk materials).”
2. How does the dopant exist in LiFePO_4 ? and by substitution in Li site or Fe site or by forming solid solution in LiFePO_4 ?

3. Why is it that a small amount of dopant can greatly improve the electrochemical performances of LiFePO_4 ? Is it due to the creation of more defects in lattice or enhancing electrochemical activity?
4. Appropriate doping of some ions in LiFePO_4 can improve the electrochemical performance, which is a well known essential fact. However, what is the dependable mechanism?

REFERENCES

1. Pier Paolo Prosini, Daniela Zane and Mauro Pasquali, 2001, *Electrochim. Acta*, 46(23), 3517.
2. Navet, N., Chouinard, Y., Magnan, J. F., Besner, S., Gauthier, M. and Arnaud, M. 2001, *J. Power Sources*, 97-98, 503.
3. Padhi, A. K., Nanjundaswamy, K. S. and Goodenough, J. B. 1997, *J. Electrochem. Soc.*, 144, 1188.
4. Kwon, S. J., Kim, C. W., Jeong, W. T. and Lee, K. S. 2004, *J. Power Sources*, 137(1), 93.
5. Yamada, A., Chung, S. C. and Kinokuma, K. 2001, *J. Electrochem. Soc.*, 148(3), A224.
6. Zhao, C. H. and Dahn, J. R. 2002, *J. Electrochem. Soc.*, 149(9), A1184-1189.
7. Tang, Z. Y. and Ruan, Y. L. 2005, *Acta Chimica Sinica (Huaxue Xuebao)*, 63(16), 1500.

8. Chung, S. Y., Jason, T. B. and Chiang, Y. M. 2002, *Nature Materials*, 1(2), 123.
9. Saiful Islam, M., Daniel J. Driscoll, Craig A. J. Fisher, and Peter R. Slater, 2005, *Chem. Mater.*, 17(20), 5085.
10. Marnix Wagemaker, Brian L. Ellis, Drik Lutzenkirchen-Hecht, Fokko M. Mulder, and Linda F. Nazar, 2008, *Chem. Mater.*, 20(20), 6313.
11. Jiezi Hu, Jian Xie, Xinbing Zhao, Hongming Yu, Xin Zhou, Gaoshao Cao, and Jiangping Tu, 2009, *J. Mater. Sci. Technol.*, 25(3), 405.
12. Xian Zhao, Xiaozhen Tang, Li Zhang, Minshou Zhao, and Jing Zhai, 2010, *Electrochimica Acta*, 55, 5899.
13. Yu Boling, and Jiang Jiaodong, 1990, *Applied Thermal Analysis*, Textile Industry Press, Beijing, 114-120.
14. Salah, A. A., Mauger, A., Julien, C. M. and Gendron, F. 2006, *Mater. Sci. Eng. B*, 129, 232.
15. Zaghbi, K., Ravet, N., Gauthier, M., Gendron, F., Mauger, A., Goodenough, J. B. and Julien, C. M. 2006, *J. Power Sources*, 163, 560.
16. Lijuan Pang, Minshou Zhao, Xian Zhao, and Yujun Chai, 2012, *J. Power Sources*, 201, 253.
17. Bard, A. J. and Faulker, L. R. 1986, *Electrochemical methods-fundamental and applications*, Gu, L. Y., Lu, M. X. and Song, S. Z. Chinese Version, Chemical Industry Publishing Company, pp. 121.
18. Qiouming Zhang, Yuqing Qiao, Minshou Zhao, and Limin Wang, 2012, *Chinese J. Inorganic Chemistry*, 28(1), 67-73.
19. Qiouming Zhang, Yuqing Qiao, Minshou Zhao, and Limin Wang, 2012, *J. the Chinese Society of Rare Earth*, 30(1), 78-85.